

Universal constraint for efficiency and power of a heat engine

Yu-Han Ma,^{1,2} Da-zhi Xu,^{3,*} Hui Dong,^{2,†} and Chang-Pu Sun^{1,2,‡}

¹*Beijing Computational Science Research Center, Beijing 100193, China*

²*Graduate School of Chinese Academy of Engineering Physics, Beijing 100084, China*

³*Center for Quantum Technology Research and School of Physics,
Beijing Institute of Technology, Beijing 100081, China*

The constraint relation for efficiency and power is crucial to design optimal heat engines operating within finite time, yet remains missing. We find a universal constraint between efficiency and output power for heat engines in low dissipation region with a phenomenological model. Such constraint is validated with an example of a Carnot-like engine. Its microscopic dynamics is governed by the master equation. Based on the master equation, we connect the microscopic coupling strengths to the generic parameters in the phenomenological model. We find the usual assumption of low dissipation is achieved with strong coupling to thermal environments. Additionally, such connection allows the design practical cycle to optimize the engine performance.

PACS numbers: to be added later

Introduction - For a heat engine, efficiency and power are the two key quantities to evaluate its performance during converting heat into useful work. To achieve high efficiency, one has to operate the engine in a nearly reversible way to avoid irreversible entropy generation. Carnot cycle is an extreme example in such manner, with which the fundamental upper bound of efficiency $\eta_C = 1 - T_c/T_h$ is achieved with infinite long operating time [1]. Such long time reduces the output power, which is defined as converted work over operating time. Generally, efficiency reduces as power increase, or vice visa. Such constraint relationship between efficiency and power is critical to design optimal heat engines. Attempts towards finding such constraint is initialized by Curzon and Ahlborn with a general derivation of the efficiency at the maximum power (EMP) $\eta_{CA}^{EMP} = 1 - \sqrt{T_c/T_h}$ [2–4]. The EMP of heat engine has attracted much attention and has been studied by different approaches, such as Onsager relation [5, 6] and stochastic thermodynamics [7, 8] with various systems [9–13]. Esposito et. al. discussed the low-dissipation Carnot heat engine by introducing the assumption that the irreversible entropy production of the finite time isothermal process is inversely proportional to time [14], and obtained a universal result of the upper and lower bounds of the EMP via optimization of the dissipation parameters.

However, a universal constraint relation between efficiency and power remains missing, though several attempts have been pursued [16–18]. In this paper, we obtain a simple constraint relation between efficiency η and output power P as

$$\tilde{\eta} + \frac{(1 - \eta_C) \tilde{P}}{2 \left(1 + \sqrt{1 - \tilde{P}} \right) - \eta_C \tilde{P}} \leq 1, \quad (1)$$

where $\tilde{\eta} \equiv \eta/\eta_C$ is the normalized efficiency with the Carnot efficiency and $\tilde{P} \equiv P/P_{\max}$ is the dimensionless power normalized with the maximum output power of

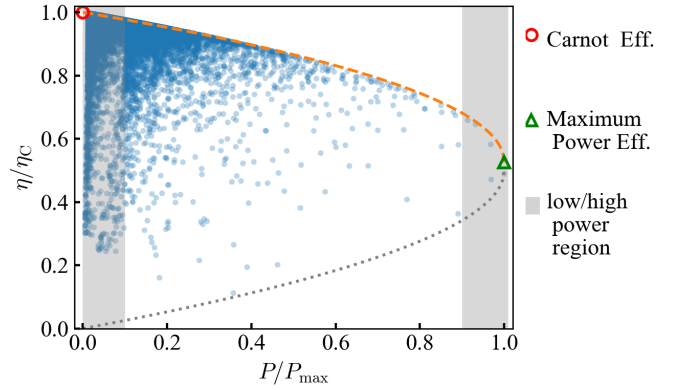


Figure 1. Constraint between normalized efficiency $\tilde{\eta} \equiv \eta/\eta_C$ and output power $\tilde{P} \equiv P/P_{\max}$. The red curve shows the constraint relation in Eq. (1). Dots show the normalized efficiency and output power of a simple two-level atomic heat engine. The gray dotted curve shows the a low-bound, which will be derived as in later discussion. The red circle denotes the Carnot efficiency η_C , which has been derived in both classical [1] and quantum system [15]. The green triangle marks the maximum power efficiency obtained in Ref. [14]. The similar bound have been derived in Ref. [17] at the limited region, shown as the gray area. Our result is valid in the whole region ($0 \leq \tilde{P} \leq 1$).

an engine P_{\max} . In the derivation, we keep temperatures of both hot and cold baths, and cycle endpoints fixed while changing only operation time. It is straightforward to show that an engine reaches the Carnot bound $\tilde{\eta} \leq 1$ at zero output power $\tilde{P} = 0$ with Eq. (1), and the efficiency at maximum power is recovered $\tilde{\eta} \leq 1/(2 - \eta_c)$ with $\tilde{P} = 1$. Our main result is illustrated in Fig. 1. We show the current up-bound of normalized efficiency $\tilde{\eta}$ as a function of the normalized output power \tilde{P} with given Carnot efficiency η_C . We note that similar constraint has been derived elsewhere [17], however only limited to extreme regions of low power $\tilde{P} \simeq 0$ and near maximum

power $\tilde{P} \simeq 1$. As shown in the derivation, the constraint is universal in the whole region $0 < \tilde{P} \leq 1$.

To validate the constraint, we present the exact efficiency and output power of a Carnot-like heat engine with a simple two-level atom as working substance. Each point in Fig. 1 shows a particular heat engine cycle with different operation time. In this example, the evolution of engine is exactly calculated via master equation, which will be shown in the later discussion. Our model connects microscopic physical parameters in the cycle to generic parameters in many previous investigations. All points follow below our constraint curve.

General derivation - In a finite time heat engine cycle, we divide the heat exchange Q_x with the high ($x = h$) and low ($x = c$) temperature baths into reversible $Q_x^{(r)} = T_x \Delta S_x$ and irreversible $Q_x^{(i)} = -T_x \Delta S_x^{(i)}$ parts, namely, $Q_x = Q_x^{(r)} + Q_x^{(i)}$, where $\Delta S_x^{(i)}$ is the irreversible entropy generated. For the reversible part, we have $\Delta S_c = -\Delta S_h$. The low dissipation assumption [14, 19–22], has been widely used in many recent studies of finite-time-cycle engines, namely

$$T_x \Delta S_x^{(i)} = \frac{M_x}{t_x}, \quad (2)$$

where t_x is the corresponding operation time. M_x is determined by the temperature T_x , the coupling constant to the bath, and the cycle endpoints, however, not dependent on operating time t_x . We will show clearly its dependence on microscopic parameters in the follow example with two-level atom. The power and efficiency are obtained simply as $P = (Q_h + Q_c)/(t_h + t_c)$ and $\eta = W/Q_h$, where $W = Q_h + Q_c$ is the converted work. Applying the inequality $a/x + bx \geq 2ab$, we have a simple relation between $Q_h^{(r)}$ and P as $\eta_c Q_h^{(r)} \geq 2\sqrt{P}(\sqrt{M_h} + \sqrt{M_c})$, which immediately leads to the maximum output power

$$P_{\max} \equiv \frac{(\eta_c Q_h^{(r)})^2}{4(\sqrt{M_h} + \sqrt{M_c})^2}. \quad (3)$$

We remark here the above inequality becomes equality only when $t_{h(c)} = \sqrt{M_{h(c)}}/P_{\max}$, which directly leads to the EMP derived in Ref. [14]. Applying the same trick solely to t_h , we obtain an inequality $P t_c^2 - (\eta_c Q_h^{(r)} - 2\sqrt{P}M_h) t_c + M_c \leq 0$, which results in a bound $t_c \in [t_c^-, t_c^+]$ with

$$t_c^\pm = \frac{\eta_c Q_h^{(r)}}{4P} \chi_c^\pm(\zeta) \quad (4)$$

for positive output power. Here, we define a nonnegative function $\chi_c^\pm(\zeta) = (\sqrt{1 - \sqrt{\tilde{P}}} \pm \sqrt{1 - \zeta\sqrt{\tilde{P}}})^2$, which depends on a dimensionless parameter

$$\zeta = \frac{\sqrt{M_h} - \sqrt{M_c}}{\sqrt{M_h} + \sqrt{M_c}} \in [-1, 1]. \quad (5)$$

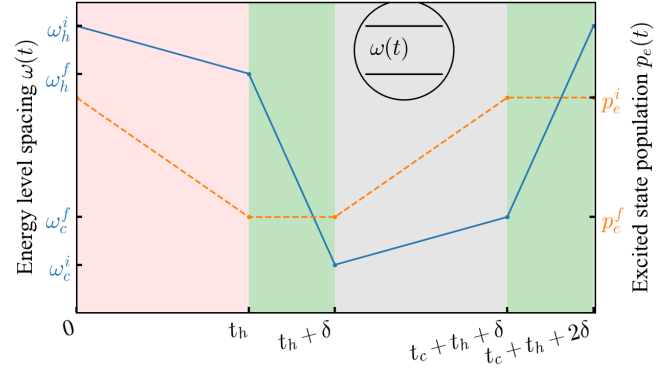


Figure 2. Carnot-like cycle with four strokes. (i) $[0 - t_h]$ quasi-isothermal process in contact with hot bath. (ii) $[t_h, t_h + \delta]$ adiabatic process. (iii) $[t_h + \delta, t_c + t_h + \delta]$ quasi-isothermal process. (iv) $[t_c + t_h + \delta, t_c + t_h + 2\delta]$ adiabatic process in contact with cold bath. The blue solid curve shows the change of energy spacing $\omega(t)$, and the orange dotted curve show the evolution of excited state population.

ζ characterizes the asymmetry of the dissipation with two heat baths. The similar result can be obtained for $t_h \in [t_h^-, t_h^+]$ by replacing the subscript $c \rightarrow h$ in Eq. (4) with $\chi_h^\pm(\zeta) = \chi_c^\pm(-\zeta)$. Noticing the monotonically increasing of efficiency η with both t_h and t_c , we obtain a upper bound for any given ζ as

$$\tilde{\eta}_+ = 1 + \frac{(1 - \eta_c)(1 + \zeta)^2 \tilde{P} + \chi_h^+ \chi_c^-}{\eta_c (1 + \zeta)^2 \tilde{P} - 4\chi_h^+}. \quad (6)$$

The overall bound of the main result in Eq. (1) is reached at $\zeta = 1$, which means $M_h \gg M_c$. Our current derivation takes advantage of only one assumption of low dissipation without specifying particular region of output power. Therefore the current result is valid in whole range $0 < \tilde{P} \leq 1$, as postulated initially in Ref. [17].

To achieve the maximum efficiency at given normalized power \tilde{P} , we adjust three parameters: the operating time t_h and t_c during contacting with both hot and cold baths, and the entropy generation ratio ζ , while fixing the temperatures T_h , T_c , and the reversible heat exchange $Q_h^{(r)}$. The derivation leaves a question about adjusting ζ , namely tuning M_h and M_c . In previous discussion, M_h and M_c are phenomenological assumed without connecting to the physical parameters. In our example of two-level atomic heat engine, tuning M_x ($x = h, c$) is achieved via changing the coupling constant of heat engine to bathes. We now switch to a specific Carnot-like quantum heat engine with two-level atom.

Validate with two-level quantum heat engine - Quantum heat engine with two-level atom is the simplest engine to illustrate the relevant physical mechanisms [23]. Here, we design a Carnot-like cycle with two-level atom, whose energy levels (the excited state $|e\rangle$ and ground

state $|g\rangle$) are tuned by the outsider agent to extract work, namely $H = \frac{1}{2}\omega(t)\sigma_z$, where $\sigma_z = |e\rangle\langle e| - |g\rangle\langle g|$ is the Pauli matrix in z-direction. The finite-time cycle consists of four strokes. Operating time per cycle is $T = t_h + t_c + 2\delta$, where t_h (t_c) is the interval of quasi-isothermal process in contact with hot (cold) bath and δ is the interval of adiabatic process. The quasi-isothermal process retains to the normal isothermal process at the limit $t_{h(c)} \rightarrow \infty$. The cycle is illustrated in Fig. 2:

(i) Quasi-isothermal process in contact with hot bath ($0 < (t \bmod T) < t_h$): The energy spacing change is linearly decreases as $\omega(t) = \omega_h^i + v_h t$, where $v_h = \epsilon_h/t_h$ is the change speed with both ω_h^i and $\omega_h^f = \omega_h^i + \epsilon_h$ fixed. The change of energy spacing is shown as solid-blue curve in Fig. 1(b). The linear change of the energy spacing is one of simplest protocol.

(ii) Adiabatic process ($t_h < (t \bmod T) < t_h + \delta$): The energy level spacing is further reduced from ω_h^f to ω_c^i , while it is isolated from any heat bath. Since there is no transition between the two energy levels, the interval δ of the adiabatic process is irrelevant of the thermodynamical quantities. In the simulation, we simply use $\delta = 0$. The heat exchange is zero, and the entropy of the system remains unchanged.

(iii) Quasi-isothermal process in contact with cold bath ($t_h + \delta < (t \bmod T) < t_h + \delta + t_c$). The process is similar to the first process, yet the energy spacing $\omega(t) = \omega_c^i + v_c(t - t_h - \delta)$ increases with speed $v_c = \epsilon_c/t_c$ and ends at $\omega_c^f = \omega_c^i + \epsilon_c$.

(iv) Adiabatic process ($t_h + \delta + t_c < (t \bmod T) < t_h + 2\delta + t_c$). The energy spacing is recovered to the initial value ω_h^i .

The two-level atom operates cyclically following the above four strokes, whose dynamics is described by the master equation

$$\frac{dp_e(t)}{dt} = -\kappa(t)p_e(t) + C(t), \quad (7)$$

where $p_e(t) \equiv \langle e|\hat{\rho}(t)|e\rangle$ is the excited state population of the density matrix $\hat{\rho}(t)$, $C(t) = \gamma(t)n[\omega(t)]$ and $\kappa(t) = \gamma(t)(2n[\omega(t)] + 1)$ with $n[\omega(t)] = 1/(\exp[\beta(t)\omega(t)] - 1)$ is the mean occupation number of bath mode with frequency $\omega(t)$. The dissipative rate $\gamma(t)$ is a piecewise function which is a constant γ_h (γ_c) during quasi-isothermal processes (i) and (iii), and zero during the two adiabatic processes. The inverse temperature $\beta(t)$ is also a piecewise function defined on quasi-isothermal process i and iii with value β_h and β_c respectively.

In the simulation, we have choose an arbitrary initial state, and perform the calculation of both efficiency and output power after the engine reaches a steady state, in which the final state of stroke (iv) matches the initial state of stroke (i). Different from the textbook Carnot cycle with isothermal process, the quantum heat engine

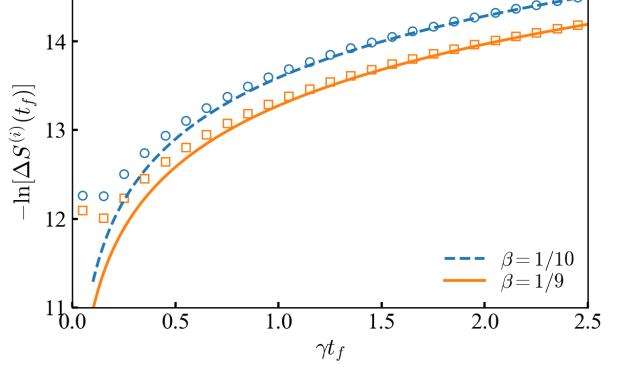


Figure 3. Irreversible entropy generation as a function of operating time at both high temperature $\beta = 1/10$ (orange) and low temperature $\beta = 1/9$ (blue). The points show the exact numerical results, and lines show the analytical results in Eq. (8).

operates away from equilibrium in the finite-time Carnot-like cycle with the quasi-isothermal process. For infinite operating time (t_h, t_c), the current cycle retains to the normal Carnot cycle.

To get efficiency and power, we consider the heat exchange and work done in two quasi-isothermal processes. The internal energy change and work done in stroke (i) is $\Delta U_h = \text{Tr}[H(t_h)\tilde{\rho}(t_h) - H(0)\tilde{\rho}(0)]$ and $W_h = \text{Tr}[\int_0^{t_h} \frac{dH(t)}{dt} \tilde{\rho}(t) dt]$, respectively. The total heat absorbed from the hot bath is given via the first law of thermodynamics as $Q_h = \Delta U_h + W_h$. The same calculation can be carried out for Q_c in stroke (iii) with the initial and final times are substituted by $t_h + \delta$ and $t_h + \delta + t_c$. The work converted and the efficiency are defined the same as in the general discussion. In our simulation, we have fixed energy spacing of the two-level atom at the four endpoints: $\omega_h^i, \omega_h^f, \omega_c^i, \omega_c^f$.

To check the upper bound, we have generated the efficiency and output power with different operating times. Each point in Fig. 1 corresponds to a set of different operating time (t_h, t_c) . In all the simulations, the operating time t_h and t_c are randomly generated. All points fall perfectly under the upper bound shown in Eq. (1).

To be comparable with the general analysis above, it is meaningful to check two key conditions: (1) low dissipation region with $1/t$ scaling of irreversible entropy production, and (2) the value of tuning parameters ζ . To check the two conditions, we firstly need calculate the irreversible entropy generation. Here, we consider a generic quasi-isothermal process starts at $t = 0$ and end at $t = t_f$ with $\omega(t) = \omega_0 + \epsilon t/t_f$. To simplify the discussion, we remove the index h and c related to the bath. The solution to Eq. (7) is formally obtained as $p_e(t) = e^{-\int_0^t \kappa(t_1) dt_1} [p_e(0) + \int_0^t e^{-\int_0^{t_1} \kappa(t_2) dt_2} C(t_1) dt_1]$, $t \in [0, t_f]$. The entropy change during the process is evaluated via von Neuman formula $S(\hat{\rho}) = -k_B \text{Tr}[\hat{\rho} \ln \hat{\rho}]$

as $\Delta S(t_f) = S(\hat{\rho}(t_f)) - S(\hat{\rho}(0))$. The irreversible entropy production in this quasi-isothermal process reads $\Delta S^{(i)} = \Delta S(t_f) - \beta Q$, where exchange Q is obtained via $Q = \Delta U + W$.

At the high temperature limit $\beta\omega(t) \ll 1$, and for $\omega_0 \gg |\epsilon|$, the irreversible entropy production (see supplemental material) reads $\Delta S^{(i)} \approx \frac{(\beta\epsilon)^2}{4\tilde{\gamma}t_f} \left(1 - \frac{1-e^{-\tilde{\gamma}t_f}}{\tilde{\gamma}t_f}\right)$, where $\tilde{\gamma} \equiv 2\gamma/(\beta\omega_0)$. At long-time limit $\tilde{\gamma}t_f \gg 1$, we keep only the leading term and get the normal assumption of $1/t$ behavior of entropy generation

$$\Delta S^{(i)} \approx \frac{(\beta\epsilon)^2}{4\tilde{\gamma}t_f}. \quad (8)$$

We plot the irreversible entropy generation as a function of contacting time t_f in Fig. 3. The points show the exact entropy generation by solving Eq. (7). At short time $\tilde{\gamma}t_f < 1$, the entropy deviates from the low dissipation region. Especially, in the extremely short contact time limit, $\lim_{t_f \rightarrow 0} \Delta S^{(i)} = (\beta\epsilon)^2/8$ is a finite quantity instead of being divergent as in $1/t$ assumption. To reach this low dissipation limit, we need either strong coupling γ between system and bath, or long-time contacting time $t_f > 1/\tilde{\gamma}$. In the simulation, we have chosen the operating time t_h and t_c to fulfill this requirement.

Back to the example of two-level atomic Carnot-like heat engine, the parameter M_x ($x = h, c$) is simply $M_x \equiv \beta_x^2 \omega_x^2 \epsilon_x^2 / (8\gamma_x)$, and γ_x is the only parameter avoidable to the tune M_x . Therefore, the dimensionless parameter ζ for whole cycle can be tuned via γ_h and γ_c . In the simulation, we have the parameter $\zeta = 0.5$, noticing all the parameters using.

We remarks that the current proof of the upper bound is based on assumption of low dissipation. Taking the two-level atomic example, the assumption is guaranteed with the long time limit $\gamma t_f \gg \beta|\epsilon|$. It is interesting to note that low dissipation can be achieved with large coupling strength γ_x to bath x , according to Eq. (8). However, it remains open to obtain the universal bound for system beyond low-dissipation region, which will be discussed elsewhere.

Beside the up-bound, we obtain a low bound for efficiency for arbitrary given output power as follow,

$$2\tilde{\eta} + \sqrt{1 - \tilde{P}} \geq 1. \quad (9)$$

The similar low bound have been derived in Ref. [16] within the framework of linear irreversible thermodynamics. The curve for low bound is illustrated as the gray dotted curve in Fig. 1. All the simulated data with two-level atom are above this curve as shown in Fig. 1. The detailed derivation for the low bound is presented in the supporting material.

Conclusion - In summary, we have derived the constraint relation between efficiency and output power of heat engine working under the so-called low dissipation

region. The constraint is valid for all the region of output power, which has not been obtained before. Importantly, we connect phenomenological parameters, used widely in many previous discussions, to the microscopic parameters, such as coupling constants to baths via a concrete example of heat engine with two-level atom. These connections enable practical adjusting the heat engine to achieve the designed function via optimizing the physical parameters, and can be experimentally verified with the state of art superconducting circuit system [24].

This work is supported by NSFC (Grants No. 11705008, Grants No. 11774323, No. 11534002), the National Basic Research Program of China (Grant No. 2016YFA0301201 & No. 2014CB921403), and the NSAF (Grant No. U1730449 & No. U1530401).

* dzxu@bit.edu.cn

† hdong@gscap.ac.cn

‡ cpsun@csirc.ac.cn

- [1] Kerson Huang, Statistical Mechanics, 2nd ed. John Wiley & Sons (1987).
- [2] F. Curzon and B. Ahlborn, Am. J. Phys. 43, 22 (1975).
- [3] P. Chambadal, Les Centrales Nucléaires, 4 (Armand Colin, Paris, 1957).
- [4] I. I. Novikov, At. Energy (N.Y.) 3, 1269 (1957); J. Nucl. Energy 7, 125 (1958).
- [5] C. Van den Broeck, Phys. Rev. Lett. 95, 190602 (2005).
- [6] S. Sheng and Z. C. Tu, Phys. Rev. E 91, 022136 (2015).
- [7] T. Schmiedl and U. Seifert, EPL. 81, 20003 (2008).
- [8] Z. C. Tu, Phys. Rev. E. 89, 052148 (2014).
- [9] Y. Izumida and K. Okuda, EPL. 83, 60003 (2008).
- [10] Z. C. Tu, J. Phys. A 41, 312003 (2008).
- [11] A. E. Allahverdyan, R. S. Johal, and G. Mahler, Phys. Rev. E 77, 041118 (2008).
- [12] B. Rutten, M. Esposito, and B. Cleuren, Phys. Rev. B 80, 235122 (2009).
- [13] M. Esposito, R. Kawai, K. Lindenberg, and C. Van den Broeck, Phys. Rev. E 81, 041106 (2010).
- [14] M. Esposito, R. Kawai, K. Lindenberg, and C. Van den Broeck, Phys. Rev. Lett. 105, 150603 (2010).
- [15] Y. H. Ma, S. H. Su, C. P. Sun. Phys. Rev. E 96, 022143 (2017).
- [16] A. Ryabov and V. Holubec, Phys. Rev. E. 93, 050101(R) (2016).
- [17] V. Holubec and A. Ryabov, J. Stat. Mech. Theory Exp. 2016, 073204 (2016).
- [18] R. Long and W. Liu, Phys. Rev. E 94, 052114 (2016).
- [19] J. Chen, J. Phys. D: Appl. Phys. 27, 1144 (1994).
- [20] A. C. Hernández, A. Medina, and J. M. M. Roco, New J. Phys. 17, 075011 (2015).
- [21] J. Gonzalez-Ayala, A. C. Hernández, and J. M. M. Roco, J. Stat. Mech. Theory Exp. 2016, 073202 (2016).
- [22] A. Dechant, N. Kiesel, and E. Lutz, EPL. 119, 50003 (2017).
- [23] H. T. Quan, Y. X. Liu, C. P. Sun, and Franco Nori, Phys. Rev. E 76, 031105 (2007).
- [24] F. Giazotto, T. T. Heikkilä, A. Luukanen, A. M. Savin, and J. P. Pekola, Rev. Mod. Phys. 78, 217 (2009).